Fractional order control of a flexible robot

Duarte Valério[1], and José Sá da Costa[1]

[1]Department of Mechanical Engineering, GCAR
Technical University of Lisbon, Instituto Superior Técnico, Lisbon, Portugal
{dvalerio,sadacosta}@dem.ist.utl.pt

Abstract — *Low robot mass / carried mass ratios make flexible robots rather attractive from the energy saving point of view, but difficulties arising from its control are significant, especially when high accuracy is needed. In this paper fractional order control for a two degree of mobility flexible robot is presented. Fractional order PID controllers with parameters tuned using genetic algorithms ensure, in simulations, a good following of trajectories, unlike integer order PID controllers, clearly less fit for such a task. Performances deteriorate in laboratory but still show fractional order control to be a promising option for this application.*

1 Introduction

A robot is said to be flexible if designed in such a manner that its structure will undergo deformation (and consequently vibration) under normal operation conditions to such a degree that rigid body models become too poor for providing suitable approximations for control. Low robot mass / carried mass ratios make flexible robots rather attractive from the energy saving point of view, but difficulties arising from its control are significant, especially for tasks demanding a high accuracy. In this paper fractional (or non-integer) order control for a flexible robot is presented. Fractional order control has been applied with success in rigid robots, both for position control and hybrid position-force control [1, 2, 3], and in a one-degree of mobility flexible robot [4]. Whenever models with significant non-linearities were used, parameter tuning was achieved either by trial and error [1] or by using a genetic algorithm [2, 3].

In what follows the application of fractional order control to a laboratory prototype of a two-degrees of mobility flexible robot, achieving a stable control-loop for the position of its tip, is described. Material is organised as follows. In section 2 a model of the robot is presented. In section 3 the implementation of fractional order controllers is addressed and genetic algorithms are shortly presented as an introduction to the genetic algorithm used in this particular case for tuning control parameters. In section 4 simulation and laboratory results are presented. Some conclusions are drawn in section 5.

2 Flexible robot addressed

The flexible robot addressed in this paper is a two-degree of mobility planar horizontal robot extant at the Control, Automation and Robotics Laboratory of the authors' Univer-

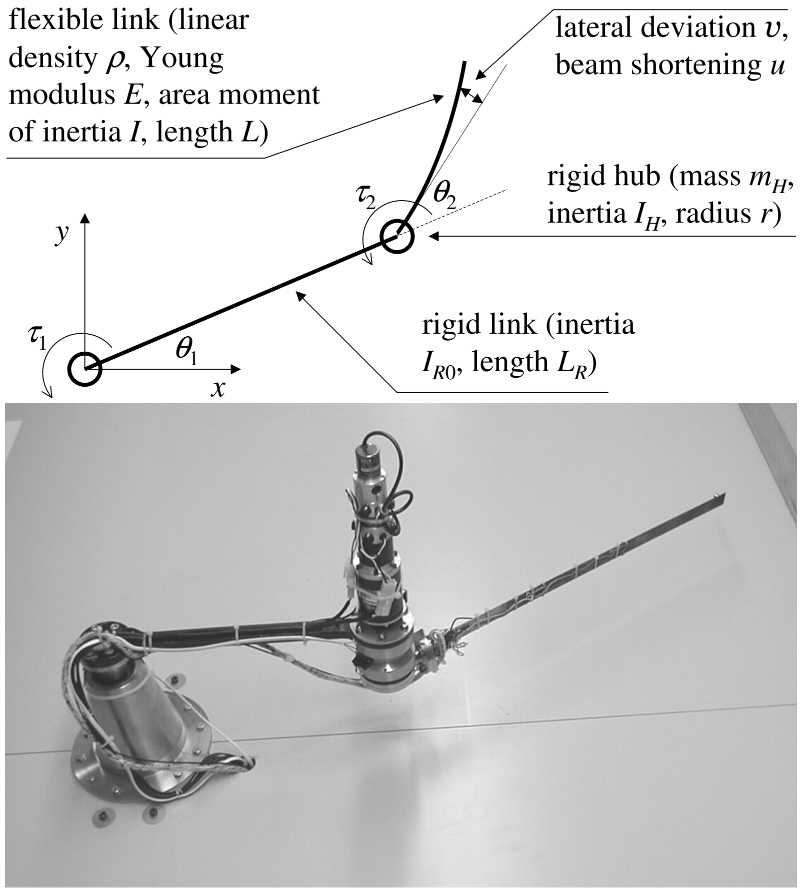

Figure 1: Flexible robotic arm addressed in this paper

sity. It consists of a rigid link and a flexible link, connected by rigid hubs, as seen in Figure 1. In each hub there are a motor, a tachometer and an encoder; the vibration of the flexible link is measured by means of two extensometer bridges. Control is performed using Matlab's xPC target toolbox. The robot's tip position can be reckoned from the two angles θ_1 and θ_2 and the elastic displacement of the flexible link v. A model of the robot, drawn from [5], is given in an Appendix.

3 Control of the robot

3.1 Fractional order controllers

Control of the position of the tip of the robot was attempted using both usual digital PID controllers and digital fractional PID controllers. The former are the weighted sum of proportional, integral and derivative control actions. The later generalise this control structure by allowing differentiation and integration orders other than 1, all real numbers being admissible. Thus five parameters are needed to define a fractional PID: the proportional, integral and derivative gains, the differentiation order, and the integration order. There are several ways for reckoning a fractional derivative or integral of a sampled signal. The one chosen stems from Tustin's formula for approximating a first order derivative, that will have to be raised to the fractional order, which we will call ν:

$$\left(\frac{2}{T}\frac{1-z^{-1}}{1+z^{-1}}\right)^{\nu} \tag{1}$$

Here T is the sampling time. Since this involves fractional powers of the delay operator z^{-1}, we expand (1) into a MacLaurin series and truncate it after some number of terms p. The result is [2, 6]

$$D^{\nu}f(t) \approx f(t)\sum_{i=0}^{p} z^{-i} \sum_{j=0}^{i} \frac{(-1)^j \left(\frac{2}{T}\right)^{\nu} \Gamma(\nu+1)\Gamma(-\nu+1)}{\Gamma(\nu-j+1)\Gamma(j+1)\Gamma(i-j+1)\Gamma(-\nu+j-i+1)} \tag{2}$$

Instead of beginning with Tustin formula, a first-order backward finite difference might have been used in (2). Or else the expected impulse response might have been used to find the coefficients of the finite impulse response filter of equation (2). Or, instead of a truncated MacLaurin series expansion, a truncated continued fraction expansion might have been used (resulting in an infinite response filter). [2, 4, 7] All these hypotheses have been tested, but the best results were obtained with (2), which was thus retained.

The control structure employed is that of Figure 2. Notice that v enters the control loop with its signal changed. This is a way of dealing with the non-minimum phase behaviour of the plant that results from the flexibility of the second link: when it turns to one side, its tip bends to the other side in a first moment [8]. Vector T contains the torques and vector q contains angles θ_1 and θ_2 and the information obtained from the extensometers (see (16), (33), (34) and (35) in the Appendix).

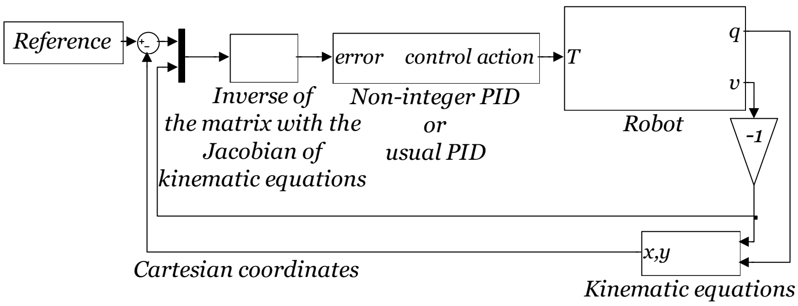

Figure 2: Control loop

3.2 Genetic algorithms

Since a genetic algorithm was successfully used in [3] for tuning the controller's parameters, this option was also adopted in this case. Genetic algorithms are an optimisation method useful in situations involving non-linearities and local minima, consisting essentially in a refined trial-and-error that imitates the evolutionary principle of the survival of the fittest [9].

The algorithm used for fitting fractional PIDs, implemented in Matlab, was as follows:

One: A population of 50 elements is created. Each corresponds to a set of two fractional PIDs, the first (C_1) for the first joint of the robot and the second (C_2) for the second

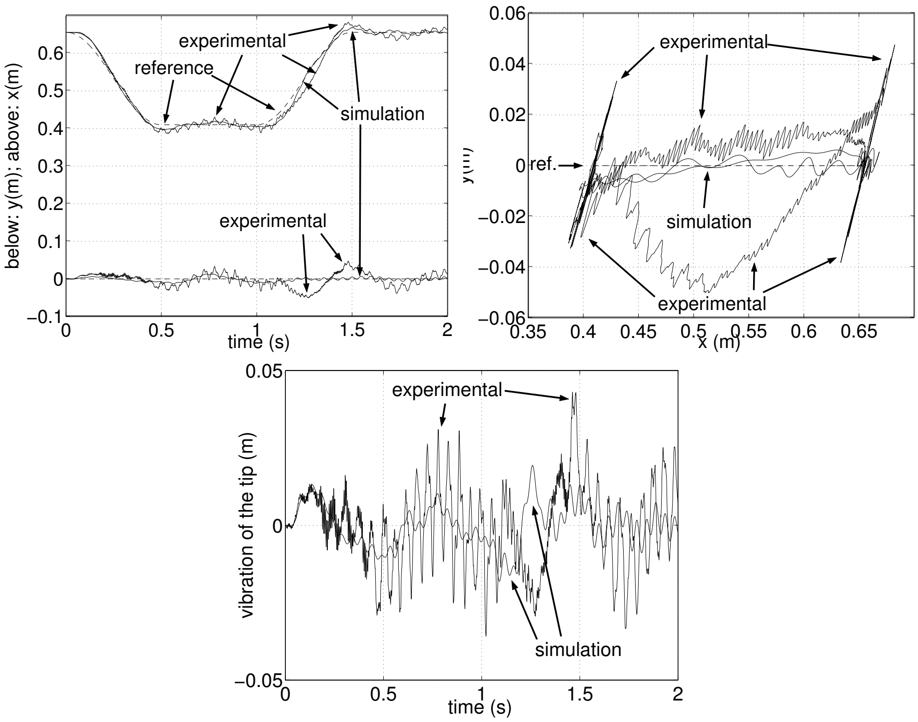

Figure 3: Control results for a linear trajectory (reference trajectory dashed)

joint, given by

$$C_1 = k_1 D^{\nu_1} + k_2 D^{\nu_2} + k_3 \tag{3}$$
$$C_2 = k_4 D^{\nu_4} + k_5 D^{\nu_5} + k_6 \tag{4}$$

Parameters, which will be stored as real numbers, are randomly chosen with normal distributions with the means and standard deviations of Table 1, which are based on previous trial-and-error tuning.

	k_1	ν_1	k_2	ν_2	k_3	k_4	ν_4	k_5	ν_5	k_6
$\overline{x}$	10^4	0	1	0	10^{-2}	10^2	0	1	0	10^{-2}
σ_x	2000	2	0.1	0.1	0.1	20	2	0.1	0.1	0.1

Table 1: Parameters' distributions

Two: Following steps are performed until 100 iterations are reached, or until no improvement arises over 10 iterations.

Three: Control is simulated for all individuals. Fractional derivatives are approximated by (2); the number of terms retained p was set to 10.

Four: A performance index is reckoned [3]. It includes the sum of the integrals of the squares of the errors in both coordinates, and a term for penalising large vibrations of the tip of the robot, since they are hard to deal with, and a potential source of inaccuracy. Vibration at the end of the simulation should be as small as possible, so

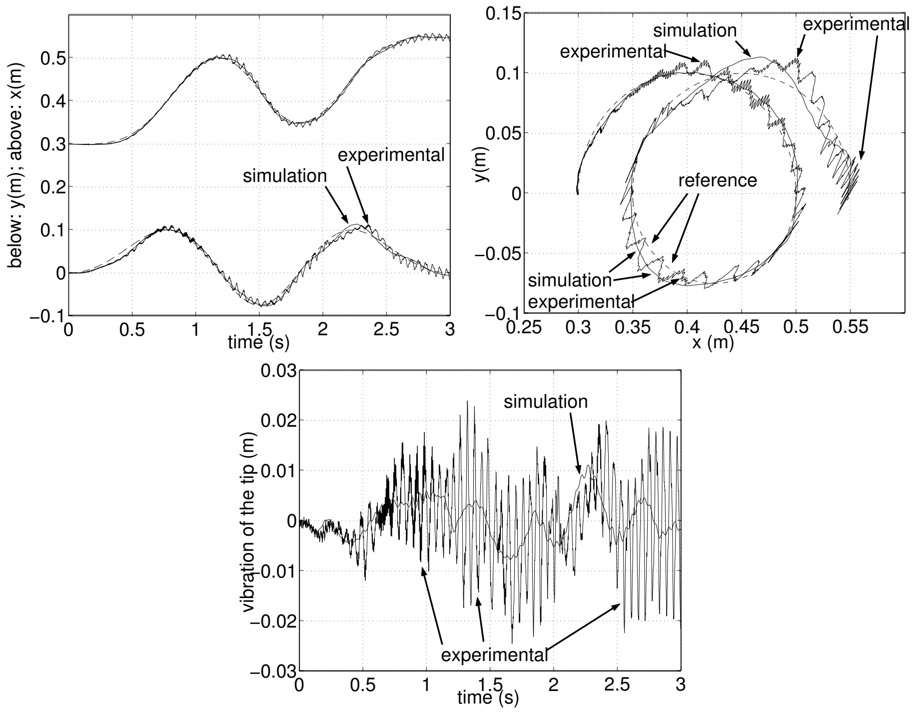

Figure 4: Control results for a two-loop trajectory (reference trajectory dashed)

that the robot may come to rest at the desired location; thus, as vibration cannot be completely avoided, it is penalised increasingly with time:

$$I = \int_0^{t_{end}} \left[(x - x_{ref})^2 + (y - y_{ref})^2 + t^2 v^4 \right] dt \tag{5}$$

Five: Eliminate all individuals save those with the 6 best performance indexes. These are allowed into the next generation (this is called elitism), and are the only ones that may reproduce or mutate.

Six: One-half of the eliminated individuals are replaced by mutations of the surviving ones. Mutants begin as copies of a randomly chosen survivor. The number of parameters that mutate is randomly chosen; the probability decreases exponentially with the number of parameters, so that it will be more likely that few parameters will change. The change consists in adding a Gaussianly distributed random number with zero-mean and variance equal to one-tenth of the mutating parameter.

Seven: One-fourth of the eliminated individuals are replaced by descendents of the surviving ones. Each descendant is the offspring of two randomly chosen survivors; each of the ten parameters listed in Table 1 is drawn, randomly, from one of the parents. Each individual being thus split into ten pieces by nine cuts, this is called nine point cross-over [9].

Eight: One-fourth of the eliminated individuals are replaced by randomly generated individuals, such as those of the original population—save that they are fewer in number. This is called spontaneous generation [3].

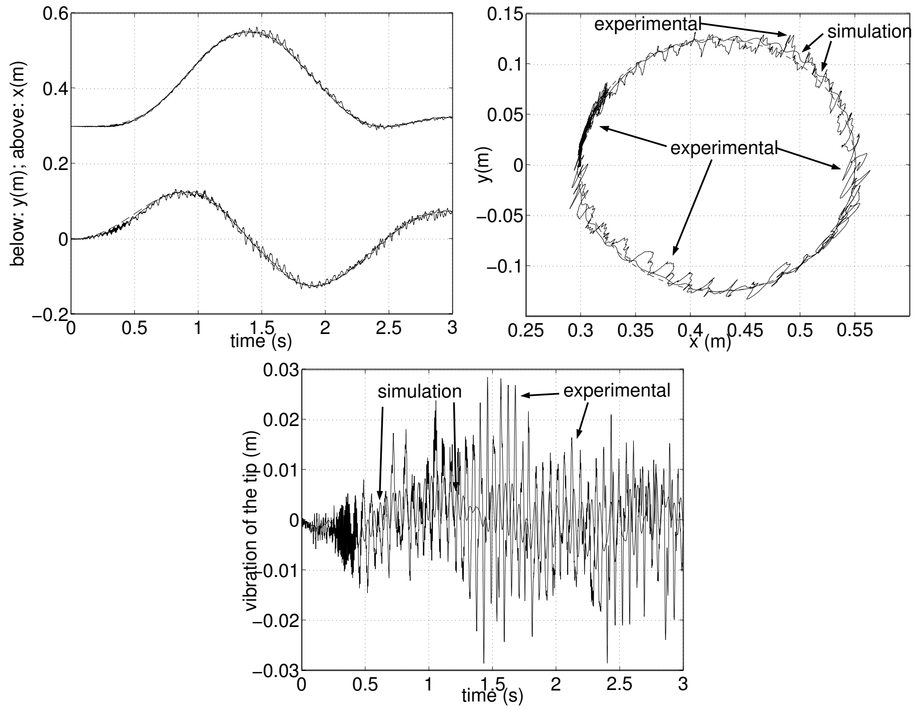

Figure 5: Control results for a circular trajectory (reference trajectory dashed)

A similar algorithm was used for fitting PIDs to the robot. The distributions given in Table 1 for parameters k_1, k_2, k_3, k_4, k_5 and k_6 were used with this algorithm as well; ν_1 and ν_4 were forced to be 1; ν_2 and ν_5 were forced to be -1.

4 Results

Three different trajectories were considered and different fractional PIDs were tuned for each. Trajectories correspond to movements usually required from robots. Figure 3, Figure 4 and Figure 5 show, for each trajectory, how the position of the tip of the robot evolves with time, the trajectory it describes in space, and the vibration it undergoes. Both simulation and experimental results are shown. The sampling time was 1 ms; controllers' parameters are given in Table 2; since only once the two available fractional derivatives were needed, the structure of the fractional PID seems to have been a reasonable choice.

Whatever the trajectory, no integer PIDs were found that could stabilise the control-loop. This does not prove, of course, that the plant cannot be controlled with integer PIDs. But the fact that no such controllers were found, while acceptable fractional PIDs were, shows that the latter are clearly superior for this application. Furthermore, controllers developed for one trajectory also work for other references as well. An example (among others possible) is shown in Figure 6, showing that controllers work for trajectories different from that they were devised for.

However, it is also clear from these results that the experimental performance is clearly worse than what was expected from simulations. Table 3 gives the half-width of an envelope around the reference trajectory that fully covers each simulation or experimental result. These envelopes are a set of circles centred on the successive points of the refer-

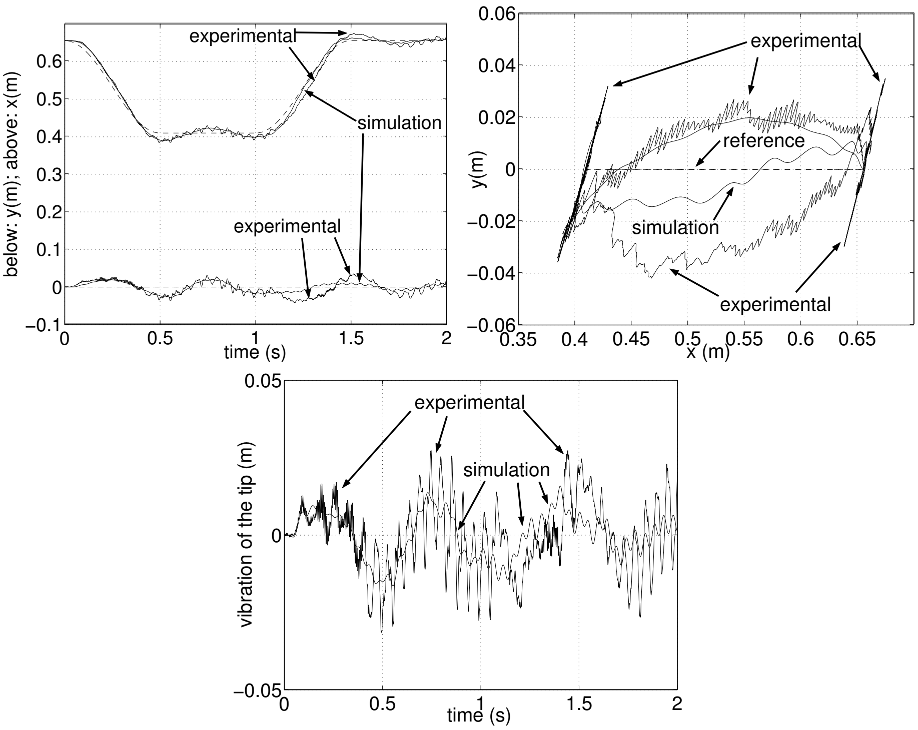

Figure 6: Control results for the trajectory of Figure 3 when the controller devised for the trajectory of Figure 2 is used

ence; their radius is the envelope half-width. Simulation values, though not good, may still be bearable, but experimental ones are clearly excessive for most applications. This is especially due to higher vibrations in experimental data and may happen because of insufficiencies in the simulation model or because of inaccurate measurements of the vibration, which is thus not properly dealt with and gets larger than it should. The model may be insufficient either in describing the vibration of the flexible link or in describing the friction in the joints. It is hard to improve the former, because taking into account more vibration modes leads to numerical problems when the kinematic equations are inverted; the latter is also hard to improve, since friction depends on temperature and on the current configuration of the robot.

It should also be noticed that fractional controllers stabilise the loop by coping with vibrations, not by suppressing them.

5 Conclusions

It was possible to control the position of the tip of the robot using fractional PIDs, while no usual (integer) PIDs able to do that could be found. Experimental results show this kind of control works, though performance is clearly poorer. These are promising results for fractional control in what concerns flexible robot control. Future work includes improving the model of the robot to attempt an increased accuracy of simulations, applying the method to more complicated robots, and refining the parameter tuning by beginning with some analytical method to find acceptable ranges for parameters and leaving the genetic

	Figure 3	Figure 4	Figure 5
k_1	4.81×10^{14}	3.89×10^{14}	59.4
ν_1	-3.63	-3.54	0.715
k_2	0	0	0
ν_2	—	—	—
k_3	0.0265	0.318	0.117
k_4	11.8	3.91×10^3	304
ν_4	0.298	-0.498	-0.114
k_5	0	1.6106	0
ν_4	—	0.0101	—
k_6	0.0929	0.400	0.0121

Table 2: Controllers' parameters

	Simulation	Experimental
Figure 3	0.016 m	0.053 m
Figure 4	0.014 m	0.021 m
Figure 5	0.006 m	0.018 m
Figure 6	0.033 m	0.042 m

Table 3: Half-width of the envelope of the reference containing simulated and experimental control results

algorithm for fine-tuning only.

Appendix

Nomenclature used in the model of the robot:

C centrifugal and Coriolis vector
E Young modulus of the robot's flexible link
F viscous friction coefficients vector
$\mathbf{H}$ mass matrix
I_b moment of inertia of the robot's flexible link
I_{m1} moment of inertia of the motor of the rigid link's joint
I_{m2} moment of inertia of the motor of joint between the two links
I_H moment of inertia of the hub connecting the links
I_{R0} moment of inertia of the robot's rigid link
$\mathbf{K}$ stiffness matrix
L length of the robot's flexible link
L_R length of the robot's rigid link
$\mathbf{M}$, $\mathbf{N}$ auxiliary matrixes
M, S auxiliary functions
T vector with the torques applied

m_b mass of the robot's flexible link, equal to ρL
m_H mass of the hub connecting the links
q time-varying vector of the coordinates that define the robot's state
r radius of the hub connecting the links
r_1 transmission relation of the rigid link's joint
r_2 transmission relation of the joint between the two links
u beam shortening in the flexible link measured longitudinally
v elastic displacement (lateral deviation) of the flexible link
α_{ij}, γ_{ij}, Φ auxiliary quantities
β_i eigenvalues corresponding to the free vibration modes of the robot's flexible link
$\eta_i(t)$ weighing coefficients called elastic coordinates
θ_1, θ_2 angles of the links
ρ linear density of the robot's flexible link
τ_1, τ_2 torques applied at the joints by motors
χ_i normalised clamped-free vibration modes

The following auxiliary quantities will be used:

$$\mathbf{M}_{i,j} = \int_r^{r+L} M(x) \frac{d\chi_i(x)}{dx}\frac{d\chi_j(x)}{dx}dx \tag{6}$$

$$\mathbf{N}_{i,j} = \int_r^{r+L} S(x) \frac{d\chi_i(x)}{dx}\frac{d\chi_j(x)}{dx}dx \tag{7}$$

$$M(x) = \int_x^{r+L} \rho d\xi \tag{8}$$

$$S(x) = \int_x^{r+L} \rho\xi d\xi \tag{9}$$

$$\gamma_{ij} = \int_r^{r+L} S(x)\chi_i(x)\frac{d^2\chi_j(x)}{dx^2}dx \tag{10}$$

$$\gamma'_{ij} = \int_r^{r+L} \frac{dS(x)}{dx}\chi_i(x)\frac{d\chi_j(x)}{dx}dx \tag{11}$$

$$\alpha_{ij} = \int_r^{r+L} M(x)\chi_i(x)\frac{d^2\chi_j(x)}{dx^2}dx \tag{12}$$

$$\alpha'_{ij} = \int_r^{r+L} \frac{dM(x)}{dx}\chi_i(x)\frac{d\chi_j(x)}{dx}dx \tag{13}$$

$$\Phi(i) = \int_r^{r+L} \chi_i(x)\,dx \tag{14}$$

$$\chi_i(x) = \cosh\left[\beta_i(x-r)\right] - \cos\left[\beta_i(x-r)\right] - \frac{\cosh(\beta_i L)+\cos(\beta_i L)}{\sinh(\beta_i L)+\sin(\beta_i L)}\left\{\sinh\left[\beta_i(x-r)\right] - \sin\left[\beta_i(x-r)\right]\right\} \tag{15}$$

Beam shortening u was neglected; elastic displacement v was approximated by a finite series

$$v(x,t) = \sum_{i=1}^{n} \chi_i(x)\,\eta_i(t) \tag{16}$$

Parameters used were as follows:

$$\begin{aligned}
L_R &= 0.32 \text{ m} && (17)\\
I_{R0} &= 0.25 \text{ kg m}^2 && (18)\\
I_H &= 13.22 \times 10^{-4} \text{ kg m}^2 && (19)\\
m_H &= 0.47 \text{ kg} && (20)\\
r &= 0.075 \text{ m} && (21)\\
L &= 0.5 \text{ m} && (22)\\
I_b &= 99 \times 10^{-4} \text{ kg m}^2 && (23)\\
\rho &= 0.157 \text{ kg/m} && (24)\\
m_b &= 0.0785 \text{ kg} && (25)\\
EI &= 0.349 \text{ N m}^2 && (26)\\
n &= 3 && (27)\\
\beta_1 &= 1.8751/L && (28)\\
\beta_2 &= 4.6941/L && (29)\\
\beta_3 &= 7.8548/L && (30)\\
F &= \begin{bmatrix} 2.0 \times 10^{-4} & 2.3 \times 10^{-4} & 0 & 0 & 0 \end{bmatrix} && (31)
\end{aligned}$$

This allows for a discrete model of the robot which is

$$\mathbf{H}(q)\ddot{q} + F\dot{q} + \mathbf{K}(q,\dot{q})q + C(q,\dot{q}) = T \tag{32}$$

where

$$\begin{aligned}
T &= \begin{bmatrix} \tau_1 & \tau_2 & 0 & \ldots \end{bmatrix}^T && (33)\\
\eta &= \begin{bmatrix} \eta_1 & \cdots & \eta_n \end{bmatrix}^T && (34)\\
q &= \begin{bmatrix} \theta_1 & \theta_2 & \eta \end{bmatrix}^T && (35)
\end{aligned}$$

Matrixes $\mathbf{H}$ and $\mathbf{K}$ are symmetric. The non-zero elements of $\mathbf{H}$, $\mathbf{K}$ and C are

$$\begin{aligned}
\mathbf{H}(1,1) &= \frac{1}{r_1^2}\Big[I_{m1} + I_{R0} + L_R^2(m_H + m_b) + I_H + I_b + \rho L \eta^T\eta \\
&\quad -2\rho L_R \sin\theta_2 \Phi^T \eta + 2\rho L_R \cos\theta_2 \int_r^{r+L} x dx - \eta^T \mathbf{N}\eta \\
&\quad -L_R \cos\theta_2 \eta^T \mathbf{M}\eta\Big] && (36)\\
\mathbf{H}(1,2) &= \frac{1}{r_1 r_2}\Big(I_H + I_b + \rho L \eta^T\eta - \rho L_R \sin\theta_2 \Phi^T\eta \\
&\quad +\rho L_R \cos\theta_2 \int_r^{r+L} x dx + \frac{L_R\cos\theta_2}{2}\eta^T\mathbf{M}\eta - \eta^T\mathbf{N}\eta\Big) && (37)\\
\mathbf{H}(2,2) &= \frac{1}{r_2^2}\Big(I_{m2} + I_H + I_b + \rho L\eta^T\eta - \eta^T\mathbf{N}\eta\Big) && (38)
\end{aligned}$$

$$\begin{aligned}
\mathbf{H}(1,j) &= \frac{1}{r_1}\left(\rho\int_r^{r+L} x\chi_{j-2}(x)\,dx\right. \\
&\quad \left.+L_R\cos\theta_2\rho\int_r^{r+L}\chi_{j-2}(x)\,dx\right),\quad 3\le j\le n &(39)\\
\mathbf{H}(2,j) &= \frac{1}{r_2}\left(\rho\int_r^{r+L} x\chi_{j-2}(x)\,dx\right),\quad 3\le j\le n &(40)\\
\mathbf{H}(3,j) &= \rho L,\quad 3\le j\le n &(41)\\
\mathbf{K}(i+2,i+2) &= EIL\beta_i^4-\dot{\theta}_1^2\left[\rho L+\gamma_{ii}+\gamma'_{ii}+L_R\cos\theta_2\left(\alpha_{ii}+\alpha'_{ii}\right)\right]\\
&\quad -\dot{\theta}_2^2\left(\rho L+\gamma_{ii}+\gamma'_{ii}\right)\\
&\quad -2\dot{\theta}_1\dot{\theta}_2\left[\rho L+\gamma_{ii}+\gamma'_{ii}+\frac{L_R\cos\theta_2}{2}\left(\alpha_{ii}+\alpha'_{ii}\right)\right],\\
&\qquad 1\le i\le n &(42)\\
\mathbf{K}(i+2,j+2) &= -\dot{\theta}_1^2\left[\gamma_{ii}+\gamma'_{ii}+L_R\cos\theta_2\left(\alpha_{ii}+\alpha'_{ii}\right)\right]\\
&\quad -\dot{\theta}_2^2\left(\gamma_{ii}+\gamma'_{ii}\right)-2\dot{\theta}_1\dot{\theta}_2\left[\gamma_{ii}+\gamma'_{ii}+\frac{L_R\cos\theta_2}{2}\left(\alpha_{ii}+\alpha'_{ii}\right)\right],\\
&\qquad 1\le i\le n\wedge 1\le j\le n\wedge i\ne j &(43)\\
C(1) &= \frac{1}{r_1}\left[\left(\rho L\eta^T-\rho L_R\sin\theta_2\Phi^T-\eta^T\mathbf{N}-L_R\cos\theta_2\eta^T\mathbf{M}\right)2\dot{\theta}_1\dot{\eta}\right.\\
&\quad +\left(\rho L\eta^T-\rho L_R\sin\theta_2\Phi^T-\eta^T\mathbf{N}+\frac{L_R\cos\theta_2}{2}\eta^T\mathbf{M}\right)2\dot{\theta}_2\dot{\eta}\\
&\quad +\left(-\rho L_R\sin\theta_2\int_r^{r+L}x\,dx-\frac{L_R\sin\theta_2}{2}\eta^T\mathbf{M}\eta\right.\\
&\quad \left.-\rho L_R\cos\theta_2\Phi^T\eta\right)\dot{\theta}_2^2+\left(-\rho L_R\sin\theta_2\int_r^{r+L}x\,dx\right.\\
&\quad \left.\left.+\frac{L_R\sin\theta_2}{2}\eta^T\mathbf{M}\eta-\rho L_R\cos\theta_2\Phi^T\eta\right)2\dot{\theta}_1\dot{\theta}_2\right] &(44)\\
C(2) &= \frac{1}{r_2}\left[\left(\rho L\eta^T+\frac{L_R\cos\theta_2}{2}\eta^T\mathbf{M}-\eta^T\mathbf{N}\right)2\dot{\theta}_1\dot{\eta}\right.\\
&\quad +\left(\rho L_R\sin\theta_2\int_r^{r+L}x\,dx+\rho L_R\cos\theta_2\Phi^T\eta-\frac{L_R\sin\theta_2}{2}\eta^T\mathbf{M}\eta\right)\dot{\theta}_1^2\\
&\quad \left.+\left(\rho L\eta^T-\eta^T\mathbf{N}\right)2\dot{\eta}\dot{\theta}_2-\dot{\theta}_1\dot{\theta}_2L_R\sin\theta_2\eta^T\mathbf{M}\eta\right] &(45)\\
C(i) &= \dot{\theta}_1L_R\sin\theta_2\rho\int_r^{r+L}\chi_{i-2}(x)\,dx,\quad 3\le i\le n &(46)
\end{aligned}$$

Beyond vector F, friction in the joints was modelled by means of a dead zone and of Coulomb and viscous friction affecting the input of each:

$$\tau_{\text{effective}}=\operatorname{sign}(\tau)\left(\mu\left|\tau\right|+\tau_0\right) \tag{47}$$

Parameters are given in Table 4. These (as well as those of vector F given in (31)) were found by minimising, using a genetic algorithm, the quadratic error of the model responses to steps and impulses.

	First joint	Second joint
Dead zone	$\begin{bmatrix} -3.2379 & 2.9129 \end{bmatrix}$ N m	$\begin{bmatrix} -0.5543 & 0.6608 \end{bmatrix}$ N m
τ_0	4.56 N m	0 N m
μ	0.2585	1.0231

Table 4: Friction parameters

Acknowledgments

Duarte Valério was partially supported by programme POCTI, FCT, Ministério da Ciência e Tecnologia, Portugal, grant number SFRH/BD/2875/2000, and ESF through the III Quadro Comunitário de Apoio. Both authors deeply appreciate significant support with the experimental setup provided by Jorge Martins and João Reis.

References

[1] J. A. T. Machado and A. Azenha. Fractional-order hybrid control of robot manipulators. In *Proceedings of IEEE International Conference on Systems, Man and Cybernetics*, pages 788–793. IEEE, 1998.

[2] D. Valério and J. Sá da Costa. Digital implementation of non-integer control and its application to a two-link robotic arm. In *European Control Conference*, Cambridge, 2003.

[3] D. Valério and J. Sá da Costa. Optimisation of non-integer order control parameters for a robotic arm. In *11th International Conference on Advanced Robotics*, Coimbra, 2003.

[4] B. M. Vinagre. *Modelado y control de sistemas dinámicos caracterizados por ecuaciones íntegro-diferenciales de orden fraccional*. PhD thesis, Universidad Nacional de Educación a Distancia, Madrid, 2001.

[5] J. Martins, M. Ayala Botto, and J. Sá da Costa. Modeling of flexible beams for robotic manipulators. *Multibody system dynamics*, 7:79–100, 2002.

[6] D. Valério and J. Sá da Costa. Time domain implementations of non-integer order controllers. In *5th Portuguese Conference on Automatic Control*, Aveiro, 2002. APCA.

[7] B. M. Vinagre, I. Podlubny, A. Hernndez, and V. Feliu. Some approximations of fractional order operators used in control theory and applications. *Fractional Calculus & Applied analysis*, 3:231–248, 2000.

[8] M. Benosman, F. Boyer, G. Le Vey, and D. Primault. Flexible links manipulators: from modelling to control. *Journal of Intelligent and Robotic Systems*, 34:381–414, 2002.

[9] J.-S. R. Jang. Derivative-free optimization. In *Neuro-fuzzy and Soft Computing*, pages 173–196. Prentice Hall, Upper Saddle River, 1997.

About the Authors

Duarte Valério received a Graduation and a Master's degree in Mechanical Engineering from the Technical University of Lisbon in 1999 and 2001. He is finishing a thesis for a doctoral degree on the application of fractional calculus to control. His research interests include software for fractional control and the extraction of electrical energy from sea-waves.

José Sá da Costa is head of the Centre of Intelligent Systems and Professor in the Mechanical Engineering Department at the Technical University of Lisbon. His main interests in research and teaching are in the area of systems and control.